REFORMED HYDRAULIC BULGING IN PROCUREMENT OF STRESS - STRAIN CURVE

ABINASH PANDA,Raajdhani Engineering College, Bhubaneswar
DR.PRADYUT KUMAR SWAIN,Aryan Institute of Engineering and Technology, Bhubaneswar
DR. KASINATH DASMOHAPATRA,NM Institute of Engineering and Technology, Bhubaneswar
Mr. BIBHUTI SABAT,Capital Engineering College, Bhubaneswar

ABSTRACT:
From old style hydraulic bulging of a circular diphagram, another strategy for recording a pressure strain bend is inferred named changed hydraulic bulging on the circle. New strategy permits more exact assurance of film pressure in the misshaping material. Supposition on the mass calculation is at this point not required since adjustment, utilizing circle as a deterrent, decides the sweep of bend required in securing of layer pressure. Performing changed hydraulic bulging upon only one test example, yields three marks of pressure strain bend. Tentatively got focuses have various strains, covering various regions; little, medium and huge disfigurements, inside a solitary trial. Utilization of the little transducer coordinated in device, empowers obtaining of power and along these lines dependable pressure procurement upon the known (round) math. Similarly, the acquired pressure strain bend can be utilized in a limited component model of the changed hydraulic bulging on the circle that is currently a work in progress

KEYWORDS: Modified hydraulic bulging, stress - strain curve, hydroforming

1 INTRODUCTION

From the experimental work on hydraulic bulging, performed on various sheet materials [1, 2] and from analytical considerations based on plasticity theory [3], the method has been constantly developing through experimental simplifications and automatization, in order to speed up stress and strain acquisition [4]. Hydraulic bulging has never attained the popularity of standard acquisition methods of true stress-strain curves such as tensile or compressive tests [5]. One of the reasons to this is dependency of the true stress upon geometrical assumptions set on bulge geometry. Many authors have conducted detailed research on geometry of the bulge and thickness distribution [6], some of the putting the emphasis on strain determination [7]. Giving more importance to the calculation of stress, led to the introduction of modified hydraulic bulging on the sphere.

2 CLASSICAL HYDRAULIC BULGING

2.1 IMPORTANCE OF KINEMATICS

Kinematics of hydraulic bulging is very important, since the stress depends on bulge geometry and kinematics. Stress is derived from membrane stress assumption [8]

$$\frac{\sigma_m}{r_m} + \frac{\sigma_c}{r_c} = \frac{p}{s} \quad (1)$$

where σ_m = meridional stress, r_m = meridional radius, σ_c = circular stress, r_c = circular radius, p = forming pressure and s = sheet thickness. Assumptions at the pole; $\sigma_m = \sigma_c = k_f$ and $r_m = r_c = r$ give stress as the function of geometry and pressure p.

$$k_f = \frac{rp}{2s} \quad (2)$$

where k_f = flow stress, r = radius at the pole. Radius at the pole can be determined in two ways

It can be calculated from known height of the bulge h and bulging diameter D [3] assuming spherical geometry of the bulge

$$r = \frac{1}{2}\left(\frac{a^2}{h} + h\right) \quad (3)$$

Radius can be calculated by measuring the coordinates of three points near the pole [4]

In classical hydraulic bulging, schematically shown in Figure 1, blank is fixed around its perimeter in a such way, that only its inner part of diameter D is plastically deformed by the pressure p.
Fixation should disable any draw in, in order to provide plane strain $\beta = 0$ around the perimeter of D. This prerequisite is theoretically taken for granted, but practically it can be completely accomplished and thus both ways of pole radius acquisition become erroneous.
Moreover neither exact deforming diameter D cannot be obtained correctly, since edge of the die at the point F has to be rounded with some radius Figure 1, in order to avoid material splitting on the sharp edge. Smaller corner

* Corresponding author: Ivana Lucica 5, HR-10000 Zagreb, CROATIA, +385 95 8936 123, marko.skunca@fsb.hr

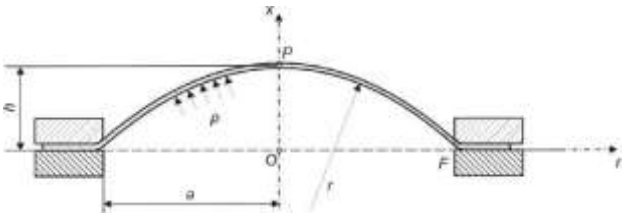

Figure 1: *Schematic representation of classical hydraulic bulging*

radius results in more accurate determination of D, enabling more precise determination of pole radius. Since minimal corner radius is material dependent, standardization of classical hydraulic bulging is not simple. It should also include the standardization of the mentioned radius. Modified hydraulic bulging completely avoids this problem.

The only prerequisites in modified hydraulic bulging are conditions that have to be met in order to have membrane stress state in the deforming sheet;

1. Sheet has to be thin regarding deforming radius; $R > 20s$
2. Meridional stress gradient has to be small
3. Change in the sheet curvature has to be moderate

All this assumptions can be found in mathematical form [8], while only the first was strictly used in construction of central part of the tooling, for 1 mm thick sheet as shown in Figure 5.

3 MODIFIED HYDRAULIC BULGING

The only difference between classical and modified hydraulic bulging is in the sphere, positioned above the deforming blank as shown in Figure 2. Deforming pressure p "pushes" sheet onto the sphere with a force F that is as acquired by the force transducer positioned in the axis of symmetry above the sphere.

3.1 STRESS AT POINT *K*

Going from the axis of symmetry x, K is the point where the sheet separates from the sphere i.e. contact and force exertion upon the sphere ceases at point K. From the geometry of the deformed blank; radius r_K, angle ϑ_K shown in Figure 3 and sheet thickness at the point K, true meridional stress $\sigma_{m,K}$ can be calculated at point K as

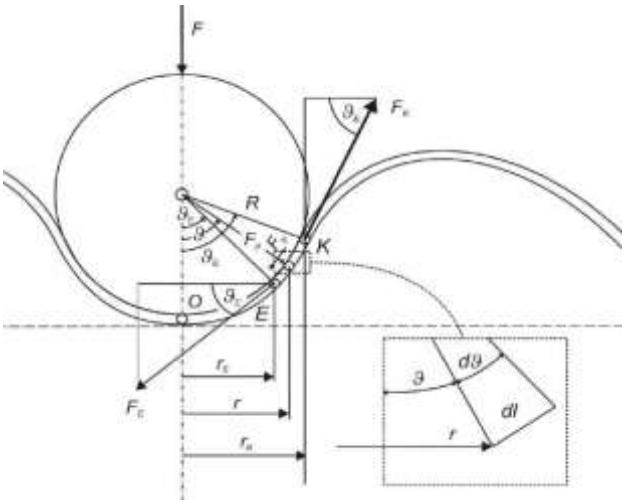

Figure 3: *Detailed representation forces and geometry in calculation of the stress at point E*

$$\sigma_{m,K} = \frac{F_K}{A_K \sin\theta_K} \quad (4)$$

where

$$F_K = F - p\,r^2\,\pi \quad (5)$$

where F = force obtained by transducer, p = deforming pressure, r_K = radius at point K (Figure 3), A_K = through-thickness surface at point K and θ_K = angle between axis of symmetry and normal at point K. Since point K lies on the sphere, radial and meridional curvature are the same, so from equation (1) circular stress $\sigma_{c,K}$ can be calculated

$$\sigma_{c,K} = \frac{p_K}{s_K} R - \sigma_{m,K} \quad (6)$$

where s_K = thickness at point K, R = radius of the sphere and p_K = contact pressure at point K calculated as

$$p_K = \frac{F}{r_K^2}\, p \quad (7)$$

where r_K = radius at point K (shown in Figure 3). Equivalent von Misses stress at point K $\sigma_{ekv,K}$ calculated from meridional and circular stress is equal to

$$\sigma_{ekv,K} = \frac{1}{} [(\sigma_{m,K} - \sigma_{c,K})^2 + (\sigma_{m,K} - \sigma_{n,K})^2 + (\sigma_{c,K} - \sigma_{n,K})^2]^{1} \quad (8)$$

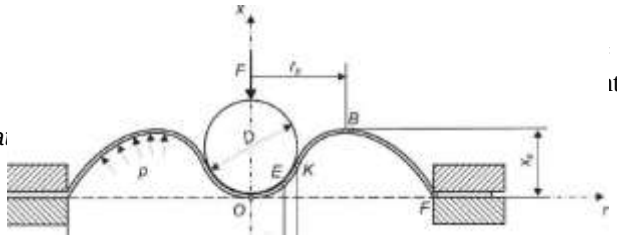

Figure 2: *Schema hydraulic bulging*

normal stress at point K calculated as mean ıtact pressure and deforming pressure p;

$$= - \frac{1}{} (\frac{F}{} + p) \quad (9)$$

$$2\ r^2 \pi$$

3.2 STRESS AT POINT *E*

Point E is the point of maximal thinning of the sheet in modified bulging. Therefore, equilibrium of forces in radial direction between points K and E gives,

$$\Sigma F_r = 0 \quad (10)$$

$$F_E \cos(\theta_E) - F_{tr} \cos(\theta) + F_p \sin(\theta) + F_K \cos(\theta_K) = 0 \quad (11)$$

resulting in force at point E calculated as

$$F_E = \frac{1}{} \cos(\theta_E)\{F_K \cos(\theta_K) - p_K R^2 \pi \mu [\cos(2\theta_K) - \cos(2\theta_E)] + 2p_K R^2 \pi \{[\theta_K - \frac{1}{2} \sin(2\theta_K)] - [\theta_E - \frac{1}{2} \sin(2\theta_E)]\}\}$$

Friction factor was taken to be $\mu = 0.2$. Division of meridional force with through-thickness area A_E at point E results in stress

$$\sigma_{m,E} = \frac{F_E}{A_E} = \frac{F_E}{\pi s_E (2r_E + s_E r_E R)} \quad (12)$$

Since point E lies on the sphere, radial and meridional curvature are the same and from equation (1) circular strain is calculated as

one of the points. Using the strain ratio $\beta = \phi_2/\phi_1$ ($\phi_1 > \phi_2$) [9], relation between equivalent and through-thickness strain is given as

$$\phi_{eq} = \frac{2}{3} \frac{\sqrt{1 + \beta + \beta^2}}{1 + \beta} \phi_3 \quad (17)$$

In modified hydraulic bulging with no draw in allowed, strain ratio β can only obtain values between 0 (plane strain) and 1 (equibiaxial stretching). Since the values of function given by Equation (17) are monotonically decreasing from value $2/\sqrt{3}\ \phi_3$ at $\beta = 0$ to the value ϕ_3 at $\beta = 1$, i.e. equivalent strain is always within the interval

$$\phi_{eq} \in [1 \ldots \sqrt{3}]\ \phi_3 \quad (18)$$

In the present case of modified hydraulic bulging on the sphere two cases of strain were considered

1. For the points K and O equibiaxial stretching $\beta = 1$ was assumed
2. For the point E plane strain $\beta = 0$ was assumed

This assumption resulted in true stress-strain curve recorded for 1 mm thick Al 99.5, shown in Figure 4

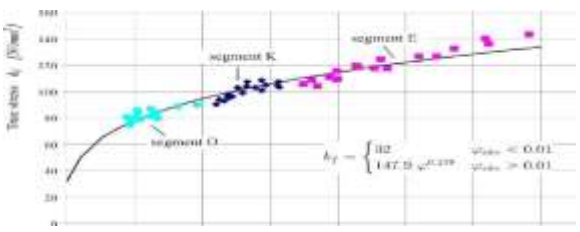

$$\sigma_{c,E} = \frac{p_K}{s_E} R \qquad (13)$$

Normal pressure at point E is the same as normal pressure at point K (see Section 3.1). So the equivalent stress at point E is given as

$$\sigma_{ekv,E} = \frac{1}{\sqrt{2}} [(\sigma_{m,E} - \sigma_{c,E})^2 + (\sigma_{m,E} - \sigma_{n,E})^2 + (\sigma_{c,E} - \sigma_{n,E})^2]^{\frac{1}{2}} \qquad (14)$$

3.3 STRESS AT POINT O

Assumption of equal meridional and circular stress at the pole $\sigma_m = \sigma_c$ (commonly used for the stress at the pole in hydraulic bulging [3]), known thickness s_O and meridional and circular radius equal to the radius of the sphere R; substituted into membrane equation (1) give in plane stress at point O as

$$\sigma_{m,c,O} = \frac{p_K}{2 s_O} R \qquad (15)$$

where p_K is same contact pressure as in Section 3.1. Normal stress at point O equals normal stress at point K in Section 3.1 so equivalent stress at point O equals

$$\sigma_{ekv,O} = |\sigma_{m,c,O} - \sigma_{n,O}| \qquad (16)$$

3.4 STRAIN IN MODIFIED BULGING

In order to record true stress-strain diagram, equivalent strain has to be determined for each one of the points K, E and O. To simplify the measurements, equivalent strain is determined from through-thickness strain at each

Figure 4: *Schematic representation of modified hydraulic bulging*

4 EXPERIMENTAL SETUP

4.1 GEOMETRY OF THE TOOLING

In order to conduct modified hydraulic bulging on the sphere, special tooling was designed and made. Bulging diameter was chosen to be D = 120 mm, radius of the corner of the die r = 5 mm and radius of the sphere R = 20.6 mm as shown in Figure 5

Acquisition of the force and geometry was performed at high pressures; from 19 bar to the limiting pressure at 24 bar. This pressure span is uniformly covered by strain ranging from 0.1 to 0.7 as follows;

- at point O strains are from 0.1 to 0.2
- at point K strains are from 0.2 to 0.3
- at point E strains are from 0.3 to 0.7

4.2 RATE OF DEFORMATION

Rate of deformation was calculated by dividing difference of strain, at point of the most intensive yielding E, for two subsequent pressures; 23 bar and 24 bar with respect to time needed for pressure to rise from 23 bar to 24 bar. Maximum rate of deformation of $\dot{\phi} = 0.25\ s^{-1}$ in modified hydraulic bulging lies on the lower boundary of the considered strain rates in the atlas of true stress - strain curves [5].

5 CONCLUSIONS

Modified hydraulic bulging on the sphere represents a new method of acquisition of true stress - strain curve. For the purpose of pre testing of the method, only one mate- rial; 1 mm thick aluminium Al 99.5 was used to record the curve shown in Figure 4.

5.1 ADVANTAGES

One great benefit of the proposed method is that; in contrast to classical hydraulic bulging, geometry of the edge of the die and die clamping diameter, both shown in Figure 5, are irrelevant for recorded true stress - strain curve. Moreover, future investigations will include stress and strain acquisition at all points from axis of symmetry to the point B shown in Figure 2.

Interesting detail to be considered is a possibility to perform modified hydraulic bulging without a force transducer, using only assumption of the membrane stress at point B. Since there is no bending stress, exerted force onto the surface of radius r_B by presure p, equals the force F on the sphere, shown in Figure 2.

For all of this purposes, a finite element model of modified hydraulic bulging on the sphere is being developed in order to support the future research.

5.2 DRAWBACKS

This method needs further development regarding; acquisition of strains larger than $\phi > 0.3$ (assumption on strain ratio β), quantitative determination regarding influence of friction onto the resulting true stress - strain curve and comparison to the results of standard methods [5].

In this paper comparison of the true stress - strain diagram

shown in Figure 4 and stress - strain diagram for Al 99.5 was not performed since only one material and one value of thickness was considered.

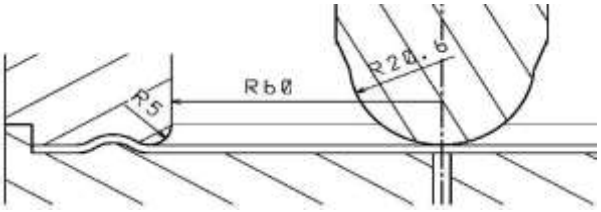

Figure 5: *Central part of the tooling; modified hydraulic bulging on the sphere*

Friction was only tested for the extremal values of $\mu = 0$ and $\mu = 0.58$ and found that it contributes very little to the stress. However, more detailed analysis is required.

Assumption on strain ratio $\beta = 0$ at point E holds only for the ultimate pressures. Since equivalent strain is additive value regarding strain path, further study of modified hydraulic bulging has to consider strain history at point E. At this moment only the upper limit of cumulative equivalent strain at point E has been assumed yielding data shown in Figure 4.

Although modified hydraulic bulging gives more direct way to acquire stress, future work has to study strain distribution in greater detail relying on available photogrammetric methods [10].

ACKNOWLEDGEMENT

This work has been supported by The Ministry of Science, Education and Sports of Republic of Croatia, within the project CAM technologies and modelling in metal form- ing and microforming.

REFERENCES

F. W. F. Brown and F. C. Thompson. Strength and failure characteristics of metal membranes in circular bulging. *Transactions of ASME*, 71: 557–585, 1949.

G. W. Panknin. The hydraulic bulge test and the determination of the flow stress curves. *Institute for Metal Forming Technology, University of Stuttgart, Germany*, 1959.

H. R. Hill. A theory of plastic bulging of a metal diaphragm by lateral pressure. *Phil. Mag*, 41: 1133–1142, 1950.

I. F. Gologranc. Untersuchungen der hydraulischen Tiefung zur Aufnahme von Fliesskurven an Blechwerkstoffen. *Anzeiger 90. Jg. Nr. 38 v. 10.*, 5: 775–779, 1968.

J. E. Doege, H. Meyer-Nolkemper, and I. Saeed. *Fliesskurvenatlas metallischer Werkstoffe*. Hanser Verlag Meunchen Wien, 1986.

K. A. Zeghloul, R. Mesrar, and G. Ferron. Influence of material parameters on the hydrostatic bulging of a circular diaphragm. *International Journal of Mechanical Sciences*, 33:229–243, 1991.

L. A. J. Ranta-Eskola. Use of the hydraulic bulge test in biaxial tensile testing. *Int. J. Mechanical Sciences*, 21:457–465, 1979.

M. I. Alfirevic. Linearna analiza konstrukcija. *Fakultet strojarstva i brodogradnje Sveuilita u Zagrebu, Zagreb*, 1999.

N. Z. Marciniak, J.L. Duncan, and S.J. Hu. *Mechanics of Sheet Metal Forming*. Butterworth-Heinemann, Woburn, 2002.

O. B. Barisic, M. Rucki, and Z. Car. Analysis of digitizing and traditional measuring system at surface measurement of lids. *Key Engineering Materials*, 381-382:217–221, 2008.